Companions around the nearest luminous galaxies: segregation and selection effects

I.D. Karachentsev[1,2,⋆] and **Y.N. Kudrya**[3]

[1] Special Astrophysical Observatory, Russian Academy of Sciences, Russia
[2] Leibniz-Institut für Astrophysik, Potsdam, Germany
[3] Taras Shevchenko National University of Kyiv, Ukraine

Received 17 November, 2014
Published online later

Key words galaxies: formation - galaxies: dwarf - galaxies: star formation

Using the "Updated Nearby Galaxy Catalog", we consider different properties of companion galaxies around luminous hosts in the Local Volume. The data on stellar masses, linear diameters, surface brightnesses, HI-richness, specific star formation rate ($sSFR$), and morphological types are discussed for members of the nearest groups, including the Milky Way and M 31 groups, as a function of their separation from the hosts. Companion galaxies in groups tend to have lower stellar masses, smaller linear diameters and fainter mean surface brightnesses as the distance to their host decreases. The hydrogen-to-stellar mass ratio of the companions increases with their linear projected separation from the dominant luminous galaxy. This tendency is more expressed around the bulge-dominated hosts. While linear separation of the companions decreases, their mean $sSFR$ becomes lower, accompanied with the increasing $sSFR$ scatter. Typical linear projected separation of dSphs around the bulge-dominated hosts, 350 kpc, is substantially larger than that around the disk-dominated ones, 130 kpc. This difference probably indicates the presence of larger hot/warm gas haloes around the early-type host galaxies. The mean fraction of dSph (quenched) companions in 11 the nearest groups as a function of their projected separation R_p can be expressed as $f(E) = 0.55 - 0.69 \times R_p$. The fraction of dSphs around the Milky Way and M 31 looks much higher than in other nearby groups because the quenching efficiency dramatically increases towards the ultra-low mass companions. We emphasize that the observed properties of the Local Group are not typical for other groups in the Local Volume due to the role of selection effects caused by our location inside the Local Group.

1 Introduction

The classical study of Dressler (1980) presented numerous observational evidence on the segregation of galaxies by morphological types: the higher the number density of galaxies, the higher among them is the fraction of early-type objects with old stellar populations, with low-gas abundances and slow star formation rates. Modern mass surveys of galaxies in different color bands like the Sloan Digital Sky Survey (Abazajian et al. 2009) have confirmed the fact, which has already become trivial that many global properties of galaxies strongly depend on the density of the environment in which the studied galaxy dwells.

There are many publications, considering the effects of segregation of galaxies in groups and clusters along their radius. There is also extensive literature which offers a variety of mechanisms to explain the observed morphological segregation: successive merging of galaxies due to the dynamical friction, sweeping out of gas from dwarf galaxies as they pass through the dense haloes of massive neighbors or through the common hot gaseous medium in clusters and groups.

There have been numerous studies in recent years examining the effects of segregation based on the data of N-body simulations (Guo et al. 2001, Hirschmann et al. 2014, Wheeler et al. 2014, Slater & Bell 2014). It is well-known that more than a half of galaxies are united in groups and clusters. A larger part of them belongs to the population of small groups, such as our Local Group. This is why the results of numerical simulations are usually compared with the observational characteristics of the Local Group (Libeskind et al. 2010, 2013, Knebe et al. 2011), considering its properties typical for the groups of galaxies in the present epoch (z = 0). However, by a number of its average parameters the Local Group significantly differs from the other neighboring groups (Karachentsev & Kudrya 2014, Karachentsev et al. 2013a). One of the major reasons of these differences is the observational selection effect conditioned by the location of the observer within the Local Group. Entwinement of the intrinsic segregations with the observational selection effect introduces distortions that must be considered when comparing the results of N-body simulations with the observational data. In this paper we try to separate the effects of segregation and selection, considering different properties of the Local Group among the number of observed characteristics of a dozen other neigh-

⋆ Corresponding author: e-mail: ikar@sao.ru

boring groups, the population and structure of which have been studied now with appropriate thoroughness.

2 The sample of nearby groups

The most complete sample of nearby galaxies, presented in the "Updated Nearby Galaxy Catalog" (= UNGC, Karachentsev et al. 2013a) contains the data on distances, D, stellar masses, M^*, hydrogen masses, M_{HI}, morphological types (de Vaucouleurs et al., 1991), T, and star formation rates, SFR, for ~ 800 galaxies located in a sphere of 11 Mpc radius. In about half of these galaxies, the distances are measured by the Hubble Space Telescope with the accuracy of at least 10%. For each UNGC-galaxy the "tidal index" Θ_1 has been determined as follows:

$$\Theta_1 = \max[\log(M^*_n/D^3_n)] + C, \quad n = 1, 2, ... N, \qquad (1)$$

which distinguishes among the plenty of nearby galaxies the most significant neighbor, whose tidal force, $F_n \sim M^*_n/D^3_n$ dominates all other neighbors. Galaxies with one common gravitationally dominant neighbor, called the "Main Disturber" = MD form a kind of a family or suite of this MD. Both physical companions of a given MD as well as distant galaxies of the general 'field' occur in this suite. The value of constant $C = -10.96$ was chosen so that $\Theta_1 = 0$ when the Keplerian cyclic period of the galaxy with respect to its MD equals the cosmic Hubble time, $1/H$. In this sense, galaxies with $\Theta_1 < 0$ may be considered as undisturbed (isolated) objects. At the same time, the set of companions with $\Theta_1 > 0$ is quite consistent with the notion of a group of galaxies around the dominant MD. Here, calculating the constant $C = -10.96$, we adopted that the total mass of each galaxy is 6 times its total luminosity in the K- band. Under such definition, the most remote members of the Local Group: Leo A, Tucana, DDO 210, and WLM have their Θ_1 just around 0, being situated near the 'zero velocity sphere' of the Local Group. It should be stressed that with this definition of a group of galaxies, no restrictions (usually subjective) were set on the difference of radial velocities and/or mutual separations of the group members (MD suite).

The principle of identification of the companions by the zones of gravitational dominance of their MDs made it possible to find in the Local Volume a lot of suites with $n = 53$ to $n = 1$ members. Their summary is presented in Table 1 (Karachentsev et al. 2014), a machine-readable version of which is available at http://lv.sao.ru/lvgdb/article/suites_dw_Table1.txt. The kinematic and dynamic properties of 15 most populous groups (suites) were discussed in detail by Karachentsev & Kudrya (2014). In general, the sizes, integrated luminosities and virial masses of these suites correspond well to the current ideas about the typical parameters of groups of galaxies.

3 The segregation of suite members by stellar masses, diameters and surface brightness.

At first, we had to exclude two groups from 15 richest suites (groups) of the Local Volume: one around IC 342 and another around NGC 6946, since both of them are located at low galactic latitudes, where it is difficult to identify dwarf spheroidal galaxies (dSph), possessing low surface brightness. The loss of statistics here was compensated by the necessary homogeneity of the sample. The remaining suites were divided into two categories: 'Early-type MD' and 'Late-type MD' according to the morphological type of their principal galaxy. To the first one we attributed groups with the MD type $T \leq 2$, where the main galaxy is dominated by a bulge. These are 5 groups (suits) around: NGC 3115 ($T = -1$),NGC 3368 ($T = 2$), NGC 4594 ($T = 1$), NGC 4736 ($T = 2$) and NGC 5128 ($T = -2$). To the second category we have attributed 6 suites with the MD type $T > 2$, where the host galaxy is dominated by a disk population. These are groups around: NGC 253 ($T = 5$), M 81 ($T = 3$), NGC 3627 ($T = 4$), NGC 4258 ($T = 4$), NGC 5236 ($T = 5$) and M 101 ($T = 6$). Two principal galaxies in the Local Group: the Milky Way ($T = 4$) and M 31 ($T = 3$) are also the disk-dominated MDs. However, we distinguished them in a separate third subsample, 'LG', because the conditions of companion search around the Milky Way and M 31 were significantly different from those at work in the remaining groups of the Local Volume.

The distribution of the companions by the projected separation R_p from the main galaxy and logarithm of the stellar mass is represented in three panels of Fig. 1. The stellar mass of galaxies was determined by their K-band luminosity, assuming the mass-to-luminosity ratio $M^*/L_K = 1 \times M_\odot/L_\odot$ (Bell et al. 2003). Physical companions of the main galaxies with the tidal indices $\Theta_1 \geq 0$ are shown by solid circles. Due to the errors in distance determination, reaching $\sim (1-2)$ Mpc at the outskirts of the Local Volume, the membership of some galaxies in groups is fragile. Therefore, we included in the consideration the likely companions of the main galaxies having slightly negative tidal indices of $\Theta_1 = (0, -0.5)$. Some of them can be real members of the groups, and the other may prove to be the general field galaxies. These objects are shown in the figure by empty squares. The upper panel of the figure corresponds to the groups, dominated by an early-type galaxy. The middle panel combines data for the groups with the main galaxies of late morphological types, and the bottom panel shows the companions of MW and M 31. Two lines with a short and long stroke show the linear regression

$$\log M^* = a \times R_p + b \qquad (2)$$

for the companions with $\Theta_1 \geq 0$ and $\Theta_1 \geq -0.5$, respectively.

The main characteristics of these groups are presented in Table 1. The upper rows of the table contain the following information: (1) the average value of logarithm of stellar mass of the group's main galaxy with the error in mean, (2)

the total number of companions with $\Theta_1 \geq -0.5$ in each category of groups, (3) the average projected separation of the companions, (4) the mean logarithm of stellar mass of companions, (5) the slope of the regression line, and its error in the case of $\Theta_1 \geq -0.5$, (6) the Fisher statistics parameter characterizing the significance of the regression slope.

The following conclusions can be drawn from these data.

- The difference in stellar masses of the main galaxies of Early-type and Late-type groups is not significant, but the masses of MW and M 31 are notably inferior to the mass of the main galaxy in the other 11 groups.
- There is no clear decrease in the mean stellar mass of companions from periphery to the center of the Early-type and Late-type groups, and only a marginally significant trend at a 2σ level is seen for the companions of the MW and M 31. Apparently, its origin is due to a selection effect, since the ultra-faint dwarfs with $\log(M^*/M_\odot) < 6$ were beyond the detection limit at large distances from the MW (Belokurov et al. 2006, Willman et al. 2009), and the zone of search for the low-mass companions around M 31 did not cover the far periphery of this group (Ibata et al. 2007, Martin et al. 2009).
- Inclusion or disregard of the companions with $\Theta_1 = (0, -0.5)$, which can conditionally be called "objects of the first infall towards the group center" do not significantly affect the slope of the regression lines.

Figure 2 shows the distribution of the companions by their Holmberg diameter A_{26} and projected separation from the main galaxy for the E-groups (the top panel), L-groups (middle one) and the Local Group (lower panel). The symbols in this figure are the same as in the previous one. The average value of logarithm of the diameter, the slope of the regression line $(a \pm \sigma)$ and the significance parameter of the slope by Fisher are presented, respectively, in rows (7–9) of Table 1. It can be concluded from the data of Fig. 2 and Table 1 that the average linear diameter of the companions decreases from periphery to the center of the group, showing the trend on $a/\sigma \sim (2-3)$ level. A similar effect is noticeable both for the companions of the MW and M 31, although it may partly be due to the above-noted selection effect. A possible physical cause of the observed trend in linear size of dwarf companions suggests a tidal stripping their outer parts, occurring in the tight vicinity of massive host galaxies (Mateo 1998, Nichols et al. 2014).

Another important parameter of galaxies is the average surface brightness (SB). In the UNGC-catalog it is determined within the Holmberg isophote 26.5 mag/sq.sec in the B-band. The distribution of the companions by their average surface brightness is shown in three panels of Fig. 3, where all the symbols are the same as in the previous figures. The mean SB of the ensemble of companions around the Early-type and Late-type MDs and around MW+M 31 are shown in line (10) of Table 1. The last two rows indicate the value of the regression slope, $a \pm \sigma$, and its statistical Fisher parameter. As one can see from these data, the surface brightness of the companions shows a brightening tendency with an increase in their projected separation. However, there is no significant trend in the E-groups, it is only pronounced at a $a/\sigma \sim 2$ level in the companions of L-groups and the LG. One reservation should be done here. In some nearby ultra-faint dwarfs, resolved into stars, their central SB often lies below the Holmberg isophote. In such cases, the average SB, presented in UNGC catalog, was estimated within the effective diameter of the dwarf, containing a half of its integral luminosity. This fact brings uncertainty in the physical interpretation of the data. Anyway, as followed from three panels of Figure 2, the most of extremely low surface brightness dwarfs, having the average SB fainter than 26.5 mag/sq.sec, occure in the neighbourhood of the Milky Way and M 31.

4 HI-richness in population of the nearby groups.

As it was shown by Haynes & Giovanelli (1984), the ratio of the neutral hydrogen mass in the galaxy to its stellar mass, M_{HI}/M^*, is significantly smaller in the central regions of clusters, as compared with the population of the general field. Subsequently, this trend of HI-richness along a radius was investigated by many authors in systems of varying degree of density and population (Cortese et al. 2008, Taylor et al. 2012, Nichols & Brand-Hawthorh 2013, Phillips et al. 2014).

The distribution of galaxies in nearby groups by ratio M_{HI}/M^* and projected separation from the main galaxy is shown in three panels of Fig. 4. The upper and middle panels correspond to the E- and L-groups, the lower panel reproduces the data for companions of the MW and M 31. The designations of galaxies are the same as in previous figures. Additionally, crosses mark the companions in which only an upper limits of HI-flux was measured. A long-stroke straight line is drawn in view of the upper limits of the HI-flux in contrast to Figures 1-3, where the line is drawn through the points with $\Theta_1 \leq -0.5$.

The data on these groups are presented in Table 2. The left columns of the data correspond to the galaxies in groups with measured HI-masses, while the right columns also include the galaxies, where only the upper limits of hydrogen masses are known. The Table 2 rows contain: (1) the total number of companions in groups of each category, (2) the average projected separation of the companions, (3) the average difference of logarithms of hydrogen and stellar mass, (4) the slope of the regression line $\log(M_{HI}/M^*) = a \times R_p + b$, where R_p is expressed in Mpc, (5) the statistical Fisher significance of the "a" parameter.

We can make the following conclusions from Figure 4 and Table 2.

- The behavior of the average M_{HI}/M^* ratio with separation from the main galaxy of the group shows the

expected deficit of HI-richness in central parts of the group. The average effect reaches a factor of $\sim (3-5)$.
– The deficit of HI-richness is more pronounced in groups, dominated by early-type galaxies. This may indicate the existence around massive E, S0, Sa-galaxies of a more extended halo of warm/hot gas, with which the interaction leads to the sweeping of neutral gas from the companions.
– Account of galaxies with the estimates of the upper limit of M_{HI} significantly enhances the observed effect.
– The correlation of M_{HI}/M^* ratio with the projected separation R_p also manifests itself for the MW and M 31 companions. As the Local Group contains much less massive companions with $\langle \log M^* \rangle = 6.3$ (see Table 1), then the sweeping of gas from them should be more effective than that in the massive companions like LMC and SMC.

5 Projected separation and star formation rate in the MD companions.

One of the most reliable indicators that allow confident division of passive and active galaxies is their specific star formation rate, $sSFR \equiv SFR/M^*$, expressed in [yr^{-1}] units. Here, the integral SFR of a galaxy is usually estimated either by the integral flux in the emission $H\alpha$ line, or by the flux in the far ultraviolet (FUV), measured by GALEX satellite (Gil de Paz, 2007). Karachentsev & Kaisina (2014) reviewed the data available in the UNGC catalog on star formation rates in galaxies of the Local Volume depending on their tidal index Θ_1. These data confirmed the known fact that the share of emission galaxies in the groups ($\Theta_1 > 0$) is significantly smaller than that of field galaxies ($\Theta_1 < 0$). Here we found it useful to develop these data not depending on Θ_1, but on the linear projected separation of companion, R_p, with respect to the main galaxy of the group. Two lower panels of Fig. 5 represent the specific star formation rate of the companions as a function of R_p for 11 nearby groups and for the companions of MW and M 31. The star formation rate for them is determined by the $H\alpha$ line flux. Two upper panels of Fig. 5 reproduce the same data calculated by the FUV flux. Symbols in Fig. 5 are the same as in the previous figure.

The average characteristics of the companions in groups of different categories are presented in Table 3. Left and right columns of the data correspond to the cases where the upper limits of the $H\alpha$ or FUV fluxes of the companions were ignored, or have been taken up as the actual values. The structure of Table 3 is similar to the previous ones. The bottom part of Table 3 reproduces the sample of companions with measured $H\alpha$ fluxes, and the upper part — that with FUV fluxes. We made a distinction between the $H\alpha$ and FUV samples, since the SFR estimates based on them have some systematic differences discussed by Pflamm-Altenburg et al. 2009, and Karachentsev & Kaisina 2014.

The following conclusions can be made from the data of Fig. 5 and Table 3.

– The effect of reducing the average specific star formation rate with decreasing separation R_p is clearly visible both in $H\alpha$ and FUV fluxes. The variation of $sSFR$ from the center to the periphery of the group reaches a factor of 10. The morphological type of the main galaxy has little effect on the amplitude of $sSFR$ trend.
– A similar, but even more remarkable variation of $sSFR$ along the radius manifests itself in the companions of MW and M 31.
– For the entire ensemble of nearby groups, including the Local Group, the dispersion of $sSFR$ in the companions increases from periphery to the group center. At the same time, as noted by Karachentsev & Kaisina (2014) and Karachentsev et al. (2013), individual $sSFR$ values do not exceed the upper limit of $\max log[sSFR] = -9.4$ yr^{-1}. The presence of this limit, as well as its value itself are important characteristics of the process of star formation in the present epoch.

6 Segregation of companions by morphological types

The above-mentioned effects of segregation of the companions by the relative abundance of hydrogen and specific star formation rate unavoidably manifest themselves in the form of morphological segregation effect, well known in the literature. Following de Vaucouleurs et al. (1991) we used, with minor modifications, such a relation between the numerical, T, and letter designation of types of galaxies: [–3, –2, –1]=[E, dSph], [0] = [S0], [1] = [S0a], [2] = [Sa], [3] = [Sab, Sb], [4] = [Sbc], [5] = [Sc], [6] = [Scd], [7] = [Sd, Sdm], [8] = [Sm], [9] = [BCD, Im], [10] = [Ir], [11] = [HI cloud].

The distribution of morphological types of companions and the projected linear separation from the main galaxy (MD) is shown in Fig. 6. Its upper and middle panels correspond to the groups, where the MD refers to the early ($T \leq 2$) or late ($T > 2$) types. The bottom panel shows the distribution of companions around MW and M 31. Physical companions with $\Theta_1 \geq 0$ are shown by solid circles, and the probable companions (or the "first infall" objects) are marked by empty diamonds. The effect of morphological segregation along the radius of group is quite clearly observed.

Table 4 reproduces the mean values, $\langle R_p \rangle$ in Mpc, for the companions, divided into 4 categories according to their morphological types: $T \leq 2, 3 \leq T \leq 8, T = 9$ and $T = 10$. The numbers in parentheses indicate the number of galaxies in each subsample. A comparison of the average $\langle R_p \rangle$ for the physical companions with $\Theta_1 \geq 0$ (left column) and companions with $\Theta_1 \geq -0.5$ (right column) show how stable are the mean values, if we additionally include in the sample probable remote companions as the "first infall" objects. Four twin columns of Table 4 correspond to

division of nearby groups according to the type of the main galaxy, which has been used above.

These data indicate that the average projected separation of the early-type companions is 2–3 times smaller than of the S-, BCD- and dIr-companions. This segregation occurs both in the groups, dominated by galaxies with dominated bulges (E, S0, Sa), and in the groups, where MD refers to the late types. The same trend is visible for the members of the Local Group, in spite of the small statistics of the late-type companions. Accounting for or ignoring of the possible companions with $\Theta_1 = (0, -0.5)$ notably affects the value of $\langle R_p \rangle$, especially for the late-type companions. In this sense, the $\langle R_p \rangle$ parameter is not quite a robust estimator of the effect of morphological segregation in groups. (Note that the trend of reduction of the average separation for the dIr-companions compared with the {BCD+Im} companions may indicate the presence among the companions with $T = 10$ of some population of tidal Holm-IX-type dwarf galaxies, which are located just beside the bright galaxies.)

Figure 7 shows the variation of the relative number of early-type companions in the nearby groups along the projected separation R_p. Solid circles and triangles correspond to groups with the main galaxy of an early- or late- type, and the solid squares mark the members of the Local Group. The intervals of the projected separation were chosen in order to provide sufficient statistics in each of them. Only the assumed physical companions with $\Theta_1 \geq 0$ were taken into account. From the analysis of these data we can draw the following conclusions.

- In general, the fraction of early-type companions around the main galaxies with dominant bulges, $f(E|E) = 33/89 = 0.37$, does not significantly differ from the relative number of early-type companions around the late-type main galaxies dominated by disks, $f(E|L) = 29/92 = 0.32$. However, the characteristic separation of early-type companions in the E-groups, ~ 350 kpc, proves to be significantly greater than in the L-groups, ~ 130 kpc. This difference likely indicates the presence in the surrounding massive E, S0, and Sa-galaxies of more extended warm gas haloes, which contribute to the transformation of star-forming irregular dwarf companions into the quenching spheroidal galaxies.
- For the companions in all 11 nearby groups, the variation of the fraction $f(E)$ along the radius is shown by empty diamonds indicating the statistical error. The $f(E)$ vs. R_p trend looks pretty smooth. It can be represented by the linear regression
$$f(E) = 0.55 - 0.69 \times R_p \quad (3)$$
(shown by the thin solid line) which goes to zero at R_p = 0.80 Mpc. This is consistent with the statement of Geha et al. (2012) that dwarf dSph galaxies with masses $\log(M^*/M_\odot) < 9$ make up not more than 0.1% among the field galaxies.
- For the MW and M 31 companions, the behavior of the $f(E)$ vs. R_p relation is significantly different from the other nearby groups. Within the $R_p = 250$ kpc radius the relative number of early-type companions in the LG exceeds 90% instead of the average value of 40% for the remaining nearby groups. This difference has an obvious explanation linked with observational selection: ultra-dwarf systems dominate among the companions of the MW and M 31. They are easily exposed to the sweep-out of gas from their shallow potential wells. A special search for such ultra-dwarfs in the vicinity of M 81 (Chiboucas et al. 2009, 2013) confirms that they are dominated by quenching objects with no signs of star formation (Kaisin & Karachentsev 2013).

7 Discussion and concluding remarks

The distribution of companions around the Milky Way and M 31 by stellar mass, linear diameter, and surface brightness reveals trends in the average values of these parameters with the projected separation from the main galaxy. The trends of the $\langle M_* \rangle$, $\langle A_{26} \rangle$ and $\langle SB \rangle$ variables of the same sign, but smaller amplitude can also be seen in the companions of 11 other neighboring groups. A comparison of the effects of segregation in the Local Group with other nearby groups indicates a significant role of the observational selection effect caused by our location inside the Local Group. This is why the observed properties of the Local Group are not typical for the remaining groups of the Local Volume. This fact should be considered when comparing the results of N-body simulations with the observational data.

In addition to the presence of ultra-faint dwarfs of extremely low surface brightness, resolved into stars only at nearby distances, the Local Group stands out among the neighboring groups by the absence in it of blue compact dwarfs (BCD), as well as HI-filaments and tidal dwarfs like Holm-IX, BK3N, Garland, A0952+69, which are visible around M 81 (Makarova et al. 2002). It should be added here that the stellar masses of MW and M 31, their virial masses, as well as the linear dimensions of the suite of companions around the MW and M 31 are notably inferior to other high-luminosity galaxies in the Local Volume.

Both the Local Group and other nearby groups show an increase towards the center of the group a fraction of early-type companions with a reduced gas abundance per unit of stellar mass, as well as a low star formation rate. The observed behavior of $\langle M_{HI}/M^* \rangle$ and $\langle sSFR \rangle$ dependences on R_p allows to check various scenarios of dynamic evolution of the companions moving inside the haloes of massive main galaxies (Kormendy & Freeman 2014, Yang et al. 2014). Based on these findings it can be assumed that the main early-type galaxies with dominant bulges possess more extended haloes composed of warm/hot gas than the disk-dominated galaxies of late types.

For the manifold of 11 most nearby and populated groups of galaxies, the relative number of passive, quenching early-type companions decreases with the projected separation as $f_E(R_p) = 0.55 - 0.69 \times R_p$, where R_p

is expressed in Mpc. Formally, this implies that beyond $R_p = 0.8$ Mpc no dwarf spheroidal companions should be present. Indeed, in the Local Group only the dwarf system Cetus with $\Theta_1 = 0.3$ and $D = 0.78$ Mpc has $R_p = 1.0$ Mpc with respect to M 31 as its host. However, in the Local Volume, there are two other examples of isolated dSph galaxies: KKR25 with $D = 1.86$ Mpc and $\Theta_1 = -1.0$ (Karachentsev et al. 2001, Makarov et al. 2012) and Apples I with $D = 8.3$ Mpc and $\Theta_1 = -1.5$ (Pasquali et al. 2005). Recently, a third very isolated dSph, KKs3, at a distance of 2.23 Mpc was found by Karachentsev et al. (2015). The search for other such quenching orphan dwarfs is an extremely painstaking observational task that can be solved in terms of deeper wide-field sky surveys in the near future.

The assumed processes involving sweeping-out of gas from the dwarf companions and locking of star formation in them while passing through the dense regions of haloes of massive neighbors manifest themselves most effectively for the companions with the smallest potential wells. Therefore, the most nearby and most studied groups in the Local Volume are the most suitable objects for the analysis of different segregation effects in them.

Acknowledgements. We are grateful to the anonymous referee for comments that helped us improve the manuscript. This work was supported by the grant of the Russian Foundation for Basic Research 13–02–90407 Ukr-f-a, and the grant of the Ukraine F53.2/15. IK acknowledge the support for proposal GO 13442 provided by NASA through grants from the Space Telescope Science Institute.

References

Abazajian, K.N., et al. 2009, ApJS, 182, 543
Bell, E.F., McIntosh, D.H., Katz, N., & Weinberg, M.D. 2003, ApJS, 149, 289
Belokurov, V., Zucker, D.B., Evans, N.W., et al. 2006, ApJL, 647, L111
Chiboucas, K., Jacobs, B.A., Tully, R.B., & Karachentsev, I.D. 2013, AJ, 146, 126
Chiboucas, K., Karachentsev, I.D., & Tully, R.B. 2009, AJ, 137, 3009
Cortese, L., Minchin, R.F., Auld, R.R. et al. 2008, MNRAS, 383, 1519
de Vaucouleurs, G. de Vaucouleurs, A., Corwin H. et al. 1991, Third Reference Catalogue of Bright Galaxies (New York: Springer)
Dressler, A. 1980, ApJ, 236, 351
Geha, M., Blanton, M.R., Yan, R., & Tinker J.L. 2012, ApJ, 757, 85
Gil de Paz, A., Boissier, S., Madore, B.F. et al. 2007, ApJS, 173, 185
Guo, Q., White, S., Boylan-Kolchin, M. et al. 2011, MNRAS, 413, 101
Haynes, M.P., & Giovanelli, R. 1984, AJ, 89, 758
Hirschmann, M., De Lucia, G., Wilman, D. et al. 2014, MNRAS, 444, 2938
Ibata, R., Martin, N. F., Irwin, M. et al. 2007, ApJ, 671, 1591
Kaisin, S.S., & Karachentsev, I.D. 2013, Ap, 56, 305
Karachentsev, I.D., Makarova L.N., Tully R.B. et al. 2015, MNRAS, 447L, 85
Karachentsev, I.D., & Kudrya, Y.N. 2014, AJ, 148, 50
Karachentsev, I.D., Kaisina, E.I., & Makarov D.I. 2014, AJ, 147, 13
Karachentsev, I.D., & Kaisina, E.I. 2014, AJ, 146, 46
Karachentsev, I.D., Makarov, D., & Kaisina E. 2013a, AJ, 145, 101 (UNGC)
Karachentsev, I.D., Karachentseva, V.E., Melnyk, O.V., & Courtois, H.M. 2013b, AstBu, 68, 243
Karachentsev, I. D., Sharina, M. E., Dolphin, A., et al. 2001, A&A, 379, 407
Knebe, A., Libeskind, N.I., Doumler, T. et al. 2011, MNRAS, 417L, 56
Kormendy, J., & Freeman, K.C. 2014, arXiv:1407.7876
Libeskind, N.I., Hoffman, Y., Forero-Romero, J. et al. 2013, MNRAS, 428, 2489
Libeskind, N.I., Yepes, G., Knebe, A. et al. 2010, MNRAS, 401, 1889
Nichols, M., Revaz, Y., & Jablonka, P. 2014, A&A, 564, 112
Nichols, M., & Bland-Hawthorn, J. 2013, ApJ, 775, 97
Makarov, D.I., Makarova, L. N., Sharina, M. E. et al. 2012, MNRAS, 425, 709
Makarova, L.N., Grebel, E.K., Karachentsev, I.D. et al. 2002, A&A, 396, 473
Martin, N. F., McConnachie, A. W., Irwin, M. et al. 2009, ApJ, 705, 758
Mateo, M.L. 1998, ARA&A, 36, 435
Pasquali, A., Larsen, S., Ferreras, I. et al. 2005, AJ, 129, 148
Pflamm-Altenburg, J., Weidner, C., & Kroupa P. 2009, MNRAS, 395, 394
Phillips, J.I., Wheeler, C., Cooper, M.C. et al. 2014, arXiv:1407.3276
Slater, C.T., & Bell, E.F. 2014, ApJ, 792, 141
Taylor, R., Davies, J.I., Auld, R., Minchin, R.F. 2012, MNRAS, 423, 787
Wheeler, C., Phillips, J.I., Cooper, M.C., Boylan-Kolchin, M., & Bullock, J.S. 2014, MNRAS, 442, 1396
Willman, B., Blanton, M.R., West, A.A. et al. 2005, ApJ, 626L, 85
Yang, Y., Hammer, F., Fouquet, S. et al. 2014, MNRAS, 442, 2419

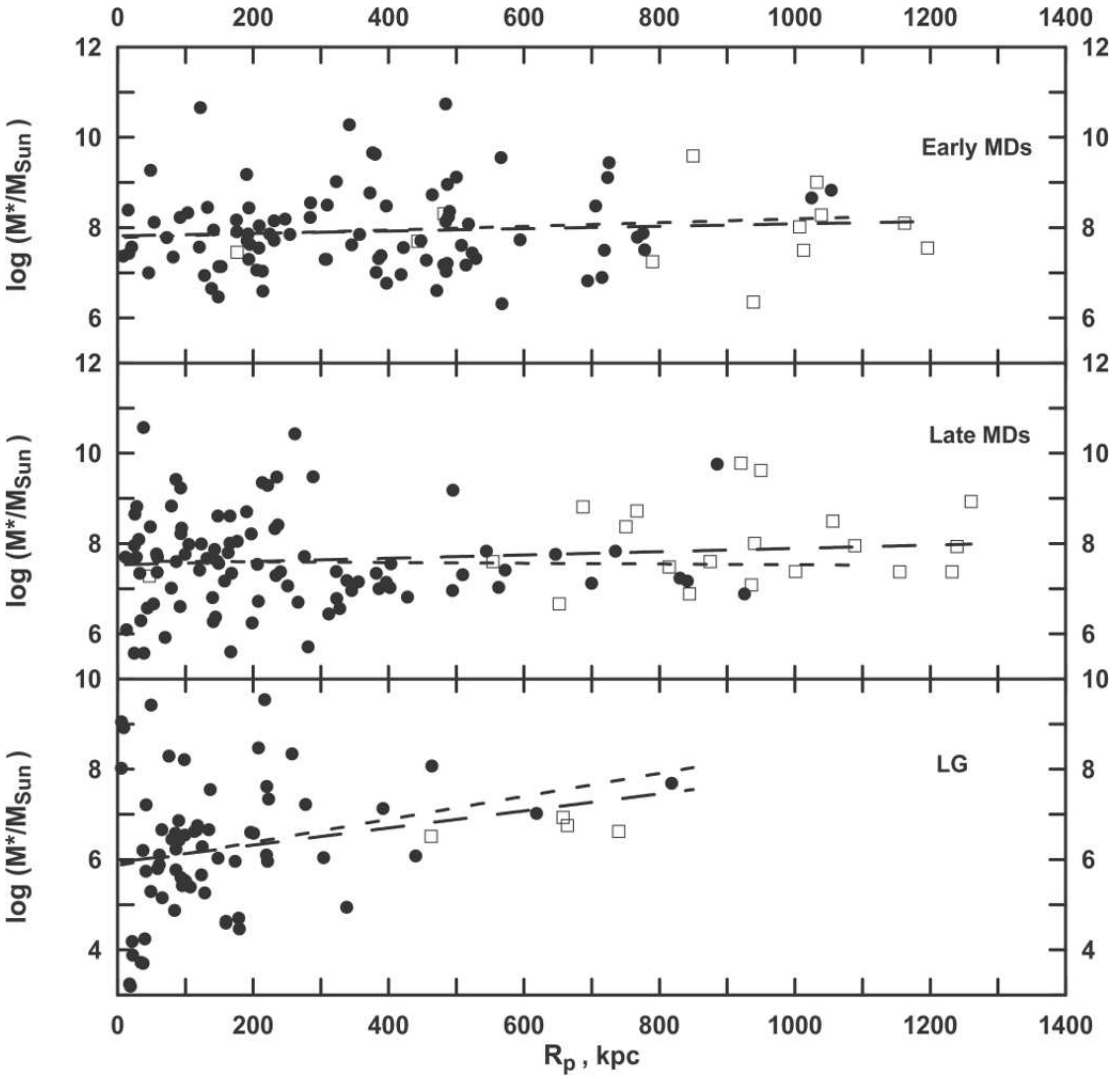

Fig. 1 The distribution of companions of nearby luminous galaxies by their stellar mass and projected separation. Solid circles represent physical companions with the tidal index $\Theta_1 \geq 0$, empty squares mark probable companions with $\Theta_1 = (0, -0.5)$. The straight line with a short stroke corresponds to the regression for the physical companions, the straight line with a long stroke — the one for the combined sample. The top panel depicts the companions around 5 massive early-type galaxies: NGC 3115, NGC 3368, NGC 4594, NGC 4736 and NGC 5128. The middle panel represents the companions around 6 massive late-type galaxies: NGC 253, M 81, NGC 3627, NGC 4258, NGC 5236 and M 101. The bottom panel — the companions of the Milky Way and M 31.

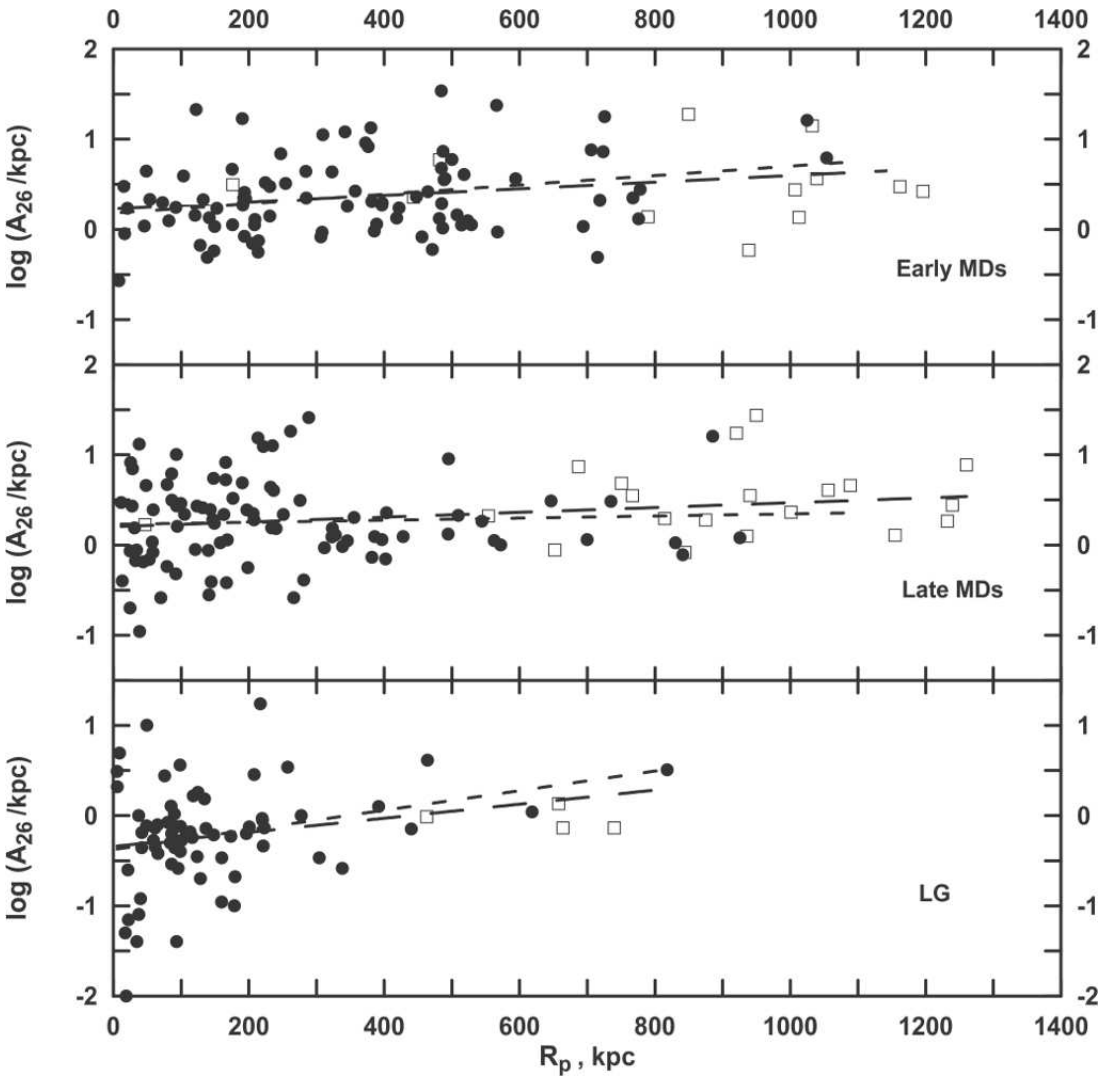

Fig. 2 The distribution of companions around nearby luminous galaxies by their linear Holmberg diameter and projected separation. The symbols are the same as in Fig. 1.

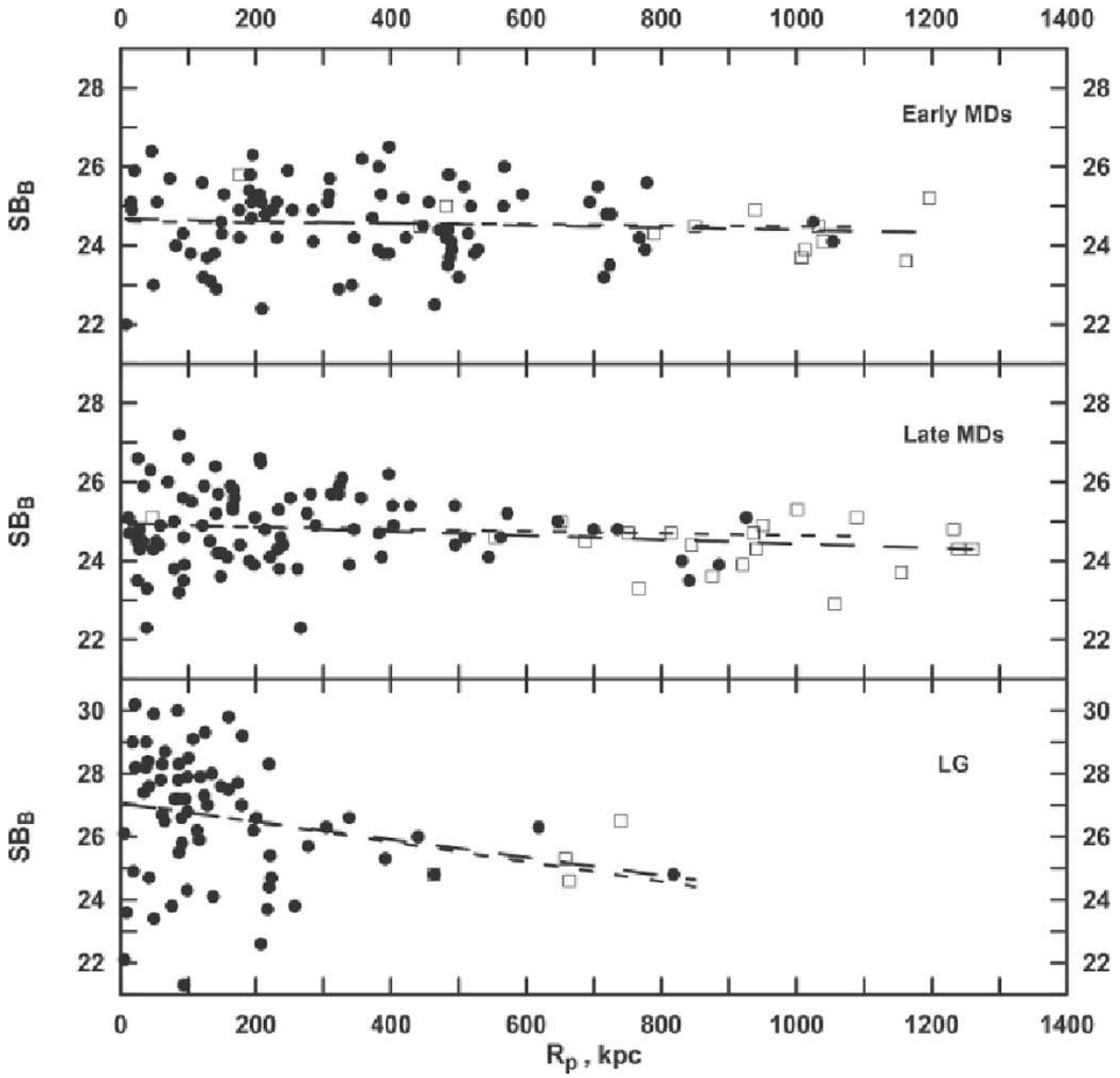

Fig. 3 The average surface brightnesses in the B-band and projected separation of companions around the nearby massive galaxies. The designations are the same as in the previous figures.

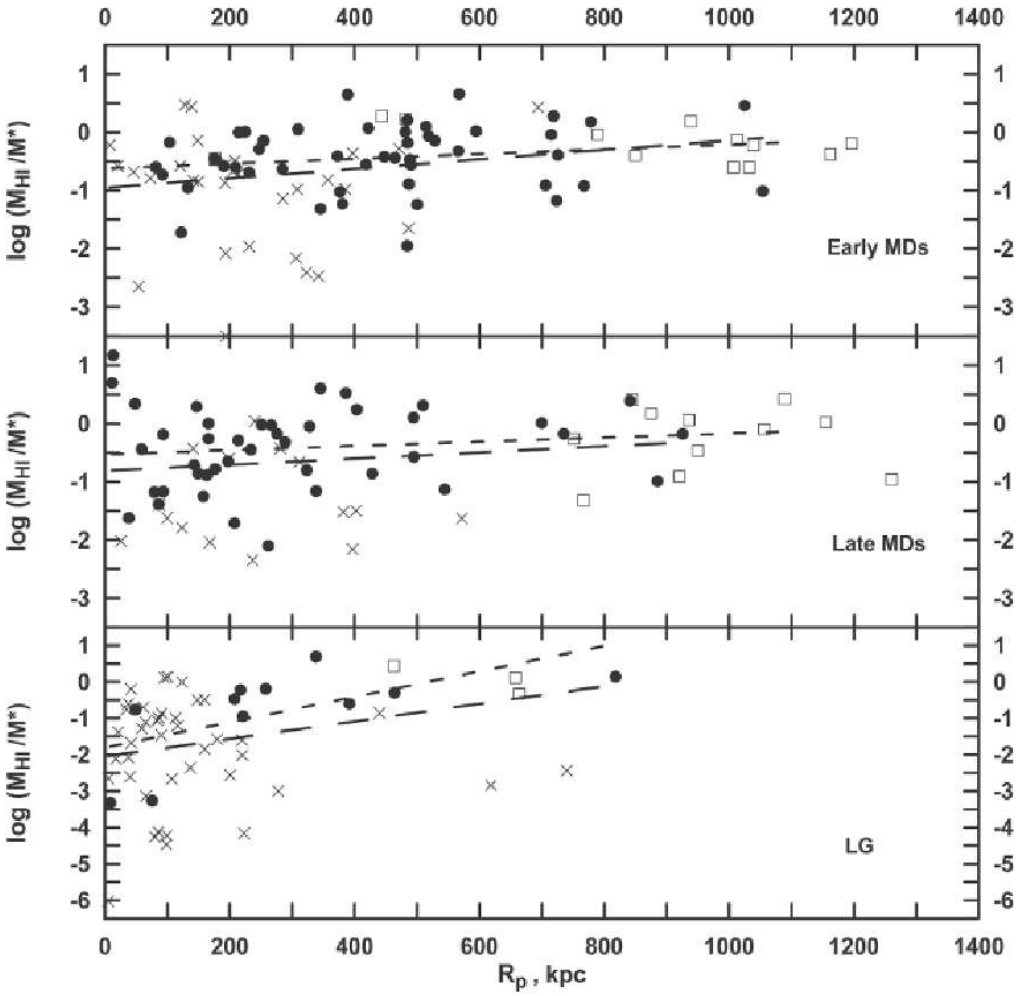

Fig. 4 The hydrogen-to-stellar mass ratio for companions of nearby bright galaxies at different projected separation from the main galaxy. The designations are the same as in the previous figures. The crosses mark the companions, in which only the top limits of hydrogen masses are measured.

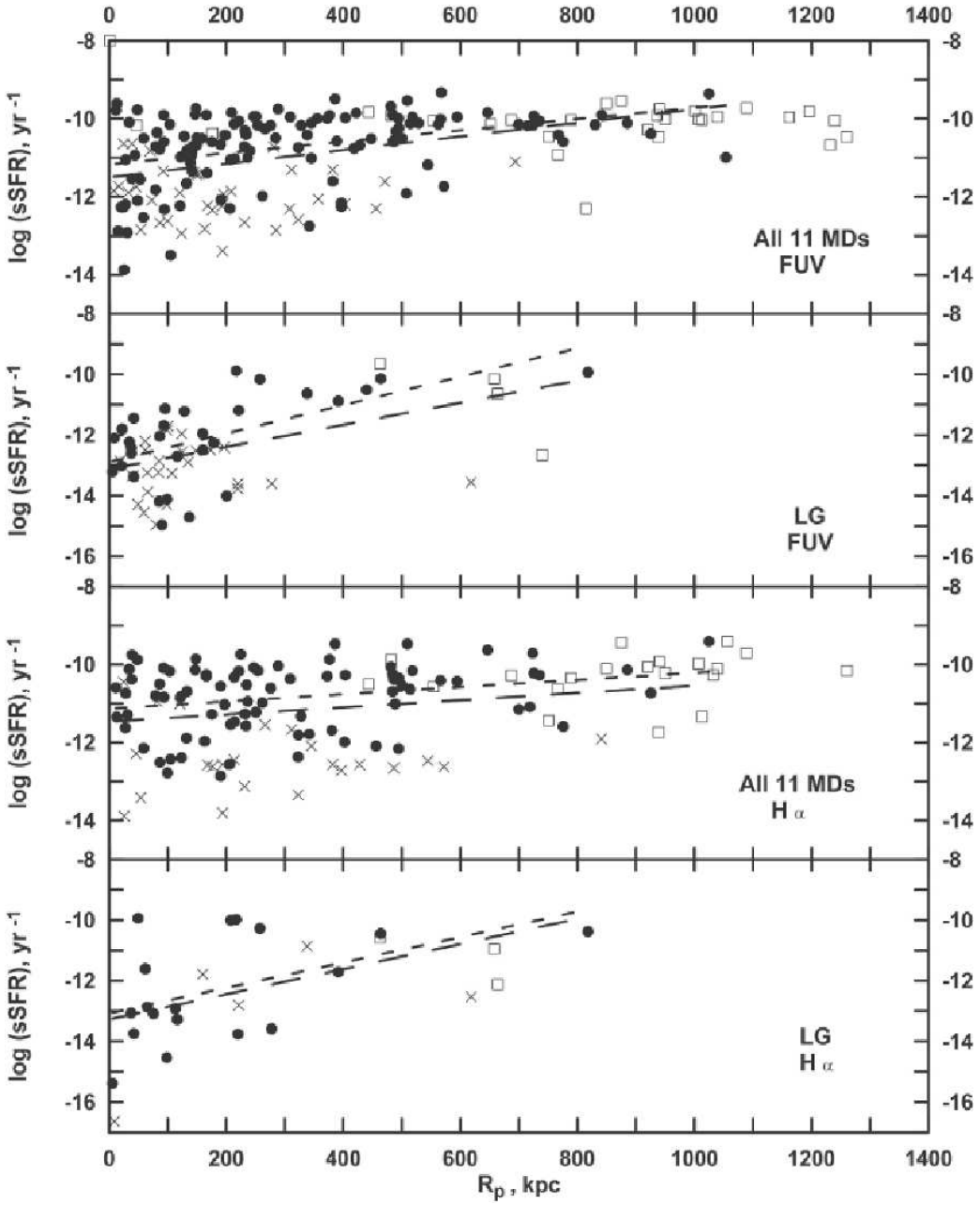

Fig. 5 Specific star formation rate vs. projected separation for the companions of nearby massive galaxies. The designations are the same as in the previous figure. The companions with estimates of the upper limit of SFR are indicated by crosses. Two lower panels represent the SFR estimates based on the $H\alpha$ line flux for the companions around 11 luminous galaxies, and for the companions of the MW and M 31. Two upper panels correspond to the SFR estimates by the FUV fluxes measured with GALEX.

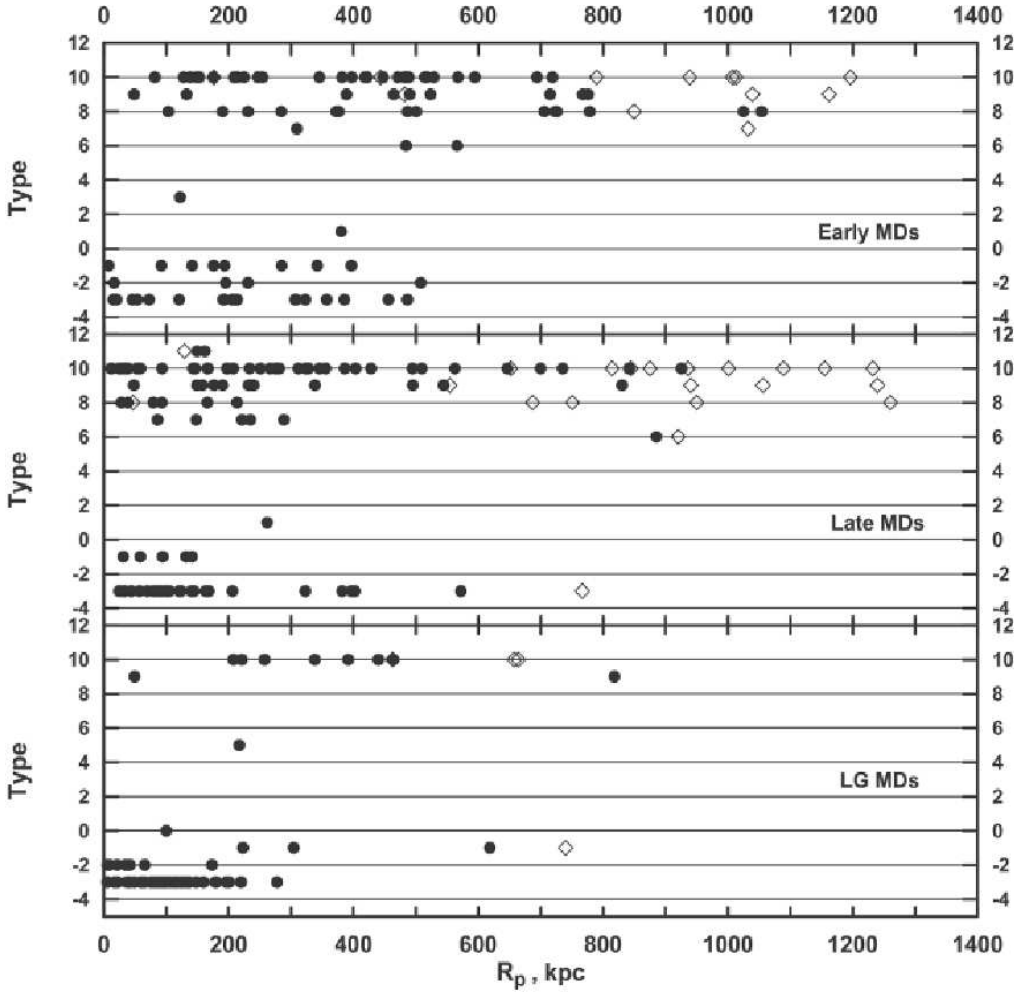

Fig. 6 Morphological type vs. projected separation for the companions around 5 luminous early-type galaxies (the top panel), around 6 luminous late-type ones (the middle panel), and around the MW and M 31 (the bottom panel). Physical companions with $\Theta_1 \geq 0$ are shown by solid circles, and probable companions having $\Theta = (0, -0.5)$ are shown by diamonds.

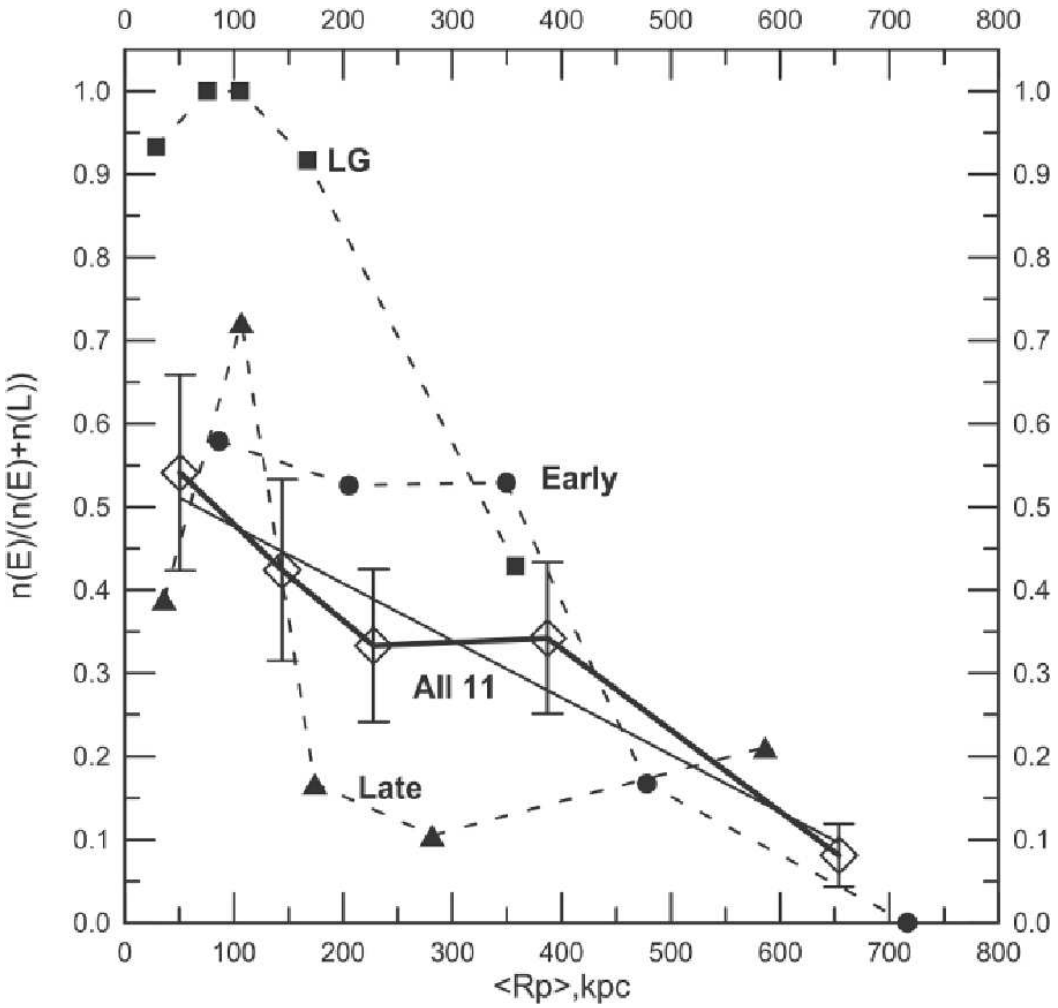

Fig. 7 The fraction of early-type companions at different projected separation around 5 massive early-type galaxies (circles), around 6 massive late-type galaxies (triangles) and around the MW and M 31 (squares). The data for companions of all the eleven early+late-type galaxies are marked with open diamonds indicating statistical errors. The regression line (3) for them is shown by thin solid line.

Table 1 The parameters of regressions $y = a \times R_p + b$ for companions around the nearby luminous galaxies, including probable companions with $\Theta_1 \geq -0.5$.

Parameter	All 11 groups	E–groups	L–groups	LG
$\langle \log M^*_{MD} \rangle$	10.93±0.07	10.92±0.11	10.94±0.03	10.72±0.02
Number	211	101	110	71
$\langle R_p \rangle$, Mpc	0.38	0.41	0.36	0.17
$\langle \log M^* \rangle$	7.79	7.93	7.66	6.27
$a \pm \sigma$	0.36±0.21	0.26±0.31	0.36±0.29	1.89±0.91
Fisher	2.84	0.71	1.59	4.29
$\langle \log A_{26} \rangle$	0.34	0.38	0.30	–0.21
$a \pm \sigma$	0.32±0.10	0.37±0.15	0.27±0.13	0.78±0.36
Fisher	10.7	6.37	4.14	4.76
$\langle SB \rangle$	24.7	24.6	24.8	26.6
$a \pm \sigma$	-0.45±0.20	–0.28±0.34	–0.53±0.25	–2.84±1.27
Fisher	4.96	0.70	4.33	4.98

Table 2 The characteristics of HI-richness for companions around the nearby luminous galaxies. The right columns in each subgroup correspond to the data taking into account the upper limit for HI-fluxes.

Parameter	All 11 groups		E-groups		L-groups		LG	
Number	112	134	59	77	53	57	14	51
$\langle R_p \rangle$, Mpc	0.48	0.33	0.53	0.36	0.44	0.29	0.35	0.16
$\langle \log(M_{HI}/M^*) \rangle$	–0.39	–0.66	–0.39	–0.66	–0.39	–0.66	–0.65	–1.68
a	0.29	0.68	0.31	0.81	0.28	0.53	3.09	2.41
Fisher	2.69	5.07	1.75	4.30	1.06	1.10	7.90	3.61

Table 3 The characteristics of the specific star formation rate (yr^{-1}) for companions around the nearby luminous galaxies of different categories. The right columns correspond to the data taking into account the upper limit of SFR. The lower part of the table corresponds to the SFR estimates by the $H\alpha$ flux and the upper part — to the SFR estimates by the FUV flux.

Parameter	All 11 groups		E-groups		L-groups		LG	
Number (FUV)	150	159	61	72	89	87	34	56
$\langle R_p \rangle$, Mpc	0.42	0.29	0.47	0.34	0.38	0.25	0.22	0.15
$\langle \log(sSFR) \rangle$	–10.60	–10.99	–10.50	–11.05	–10.67	–10.95	–11.94	–12.57
a	1.08	1.75	1.19	2.12	0.99	1.64	3.53	3.64
Fisher	28.5	29.5	16.0	22.9	12.9	11.8	13.9	12.1
Number($H\alpha$)	102	105	39	40	63	65	21	23
$\langle R_p \rangle$, Mpc	0.42	0.31	0.53	0.37	0.36	0.27	0.25	0.21
$\langle \log(sSFR) \rangle$	–10.74	–11.19	–10.56	–11.08	–10.85	–11.25	–12.11	–12.40
a	0.91	0.92	0.25	1.95	1.12	0.22	3.39	4.15
Fisher	13.4	4.09	0.44	6.74	11.3	1.35	5.75	5.80

Table 4 The average projected separation for the companions having different morphological types.

	The mean projected separation (Mpc)							
Companion type	All 11 groups		E-groups		L-groups		LG	
$T < 3$	0.19	0.20	0.22	0.22	0.16	0.18	0.11	0.12
	(61)	(62)	(32)	(32)	(29)	(30)	(58)	(59)
$2 < T < 9$	0.38	0.47	0.50	0.55	0.21	0.39	0.22	0.22
	(30)	(38)	(18)	(20)	(12)	(18)	(1)	(1)
$T = 9$	0.38	0.51	0.48	0.58	0.30	0.46	0.43	0.43
	(21)	(28)	(9)	(12)	(12)	(16)	(2)	(2)
$T = 10$	0.33	0.44	0.37	0.45	0.30	0.43	0.33	0.41
	(67)	(83)	(30)	(37)	(37)	(46)	(7)	(10)

